



Removal of cadmium(II) ions using *Saccharomyces cerevisiae* and *Leuconostoc mesenteroides* immobilized in silica materials by two processing methods

Slobodanka Stanojević-Nikolić^{a,c*} , Katarina V. Pavlović^b, Milan P. Nikolić^c , Vladimir V. Srdić^a,
Marina Šćiban^a

^aUniversity of Novi Sad, Faculty of Technology Novi Sad, Novi Sad, Serbia.

^bUniversity of Belgrade, Faculty of Biology, Belgrade, Serbia.

^cUniversity of Kragujevac, Faculty of Agronomy Čačak, Laboratory for Technological Processes Control and Sustainable Development, Čačak, Serbia.

Received: November 07, 2021; Revised: February 10, 2022; Accepted: March 22, 2022

Two processing methods for preparation of microbial biomass-silica biosorbent to remove cadmium ions from aqueous solution were developed. The first method involved a slow addition of sulphuric acid into previously prepared dispersion of viable *Saccharomyces cerevisiae* or *Leuconostoc mesenteroides* biomass in sodium silicate solution. The obtained material was mesoporous with irregular shape and size between 1 and 10 μm . The second method for the immobilization of microbial biomass by silica gel entrapment was developed in order to restrict desorption of microbial cells and to obtain larger particles with uniform size. The obtained particles were spherical with average particle size of 1.5 mm. Both materials with viable *L. mesenteroides* cells displayed higher removal efficiency compared the efficiency of materials that containing viable *S. cerevisiae* cells. Infrared spectra revealed an intensive secretion of dextran by *Leuconostoc mesenteroides* cells in the presence of cadmium ions. EDS maps clearly showed the dispersion of cadmium in the cross-section of microbial biomass-silica biosorbent. The maximum theoretical binding adsorption capacity for the silica-alginate-*S. cerevisiae* composite was 54 mg/g. The adsorption capacity for the silica-alginate-*L. mesenteroides* composite obtained after 24 cycles was about 93 mg/g. The extracellular secretion of dextran by *L. mesenteroides* cells immobilized in silica-alginate composite enabled efficient removal of cadmium ions. The efficiency of Cd(II) removal by microbial composite was not affected by the presence of co-existing ions at initial cadmium concentration of 1 and 4 mmol/L.

Keywords: Biosorption, heavy metals, silica, composite, microbial cells.

1. Introduction

Global industrialization and urbanization are responsible for increasing amounts of toxic pollutants in the effluents and soil. Environmentally relevant most hazardous substances which contaminate environment, especially water, are heavy metals, due to their persistent, non-biodegradable, and toxic nature¹. Cadmium is highly toxic, non-essential heavy metal which may cause serious health problems to all living organisms². Due to its ability to be accumulated in living organisms, it has harmful impact on lungs, kidneys, liver, reproductive organs etc. Both short-term or long-term exposure to cadmium can cause serious health problems such as renal and hepatic dysfunction, pulmonary edema, testicular damage. Also, these types of exposure can cause osteomalacia, damage to the adrenals and hemopoietic system³, as well as coronary heart disease, stroke, peripheral artery disease and atherogenic changes in lipid profile⁴. According to IARC (International Agency for Research of Cancer) cadmium is classified into the first group of metals which may cause cancer⁴. Thus, it is very important to prevent cadmium from getting into the environment from

industrial effluents. It is well known that both geogenic and anthropogenic sources can elevate Cd concentrations in soils and groundwater. Significant sources of natural Cd emissions are hydrothermal vents, weathering of rocks and airborne soil particles from deserts, sea spray, forest fires, biogenic material and volcanoes. Sources of anthropogenic Cd emissions are non-ferrous metal production, fossil fuel combustion, phosphate fertilizer manufacturing, iron, steel, and cement production and road dust. Municipal and sewage sludge incineration can also release cadmium into air, water, and soil⁵. Furthermore, Cd can be found in products such as pigments, coatings, platings, stabilizers for polyvinyl chloride (PVC) and alloys.

It has been found that phosphate fertilizers contain between 36 and 77 mg Cd per kg P_2O_5 , making them one of the most important sources of Cd contamination in soils. While the average usage of phosphate in Europe is 43 kg/(ha*a)⁵, the average value of fertilizer consumption for Serbia during the period of 2006-2018 was 143.3 kg per hectare of arable land. Phosphate fertilizers may be among main inputs of Cd in Serbia, since arable land in Serbia was reported at 29.53% in 2018.

*e-mail: slobodankasnikolic@gmail.com

Since biomass ash is often used as a fertilizer⁵ and since cadmium concentration in it can reach up to 30 mg/kg, this ash can provide an additional increase of Cd concentrations in soil.

Since the mineral industry in Serbia is dominated by copper production, pollution assessment of cadmium in agricultural soils around copper mining area may exceed the grade limit of the soil quality standard⁶. Other mineral and mineral-based commodities produced in Serbia that include cement and coal are also an important source of cadmium contamination in soil, water and air.

The application of biosorption for removal of heavy metals from wastewater has been considered as an effective procedure for water treatment⁷. Major advantages of biosorption over conventional treatment methods (precipitation, adsorption, reduction, coagulation, and membrane filtration) is low cost, eco-friendliness, high binding ability, high efficiency of removal metal ions in low concentration, low biological sludge, etc⁸. Low cost and eco-friendly biosorption of heavy metal ions using nonpathogenic microbial biomass is generally regarded as safe and it is receiving more attention in recent years⁹. The application of these biosorbents for wastewater treatment may easily be globally accepted and eventually widely used in practice in the field of biosorption¹⁰.

Biomass used for biosorption may be either viable or not. The use of non-viable biomass is usually considered easier because it is less complex than viable one, and due to absence of influence of metabolic processes on sorption, which is usually considered inappropriate¹¹. The use of non-viable biomass enables numerous advantages such as: absence of toxicity limitations; absence of requirements for growth medium and nutrients in the feed solution; easy absorbance and recovery of biosorbed metals; easy regeneration and reusability of biomass; possibility for easy immobilization of dead cells; easier mathematical modelling of metal uptake¹².

Despite obvious advantages of using non-viable biomass over living microorganisms, in some instances living microorganisms are more useful. For example, the reduction of Cr⁶⁺ to less toxic Cr³⁺ can be performed by processes mediated by living bacteria^{9,13}. The biosorption of heavy metals using live biomass of bacterial cells (*Brevundimonas species* IITISM22) allows intracellular adhesion of functional group to Hg (II). Furthermore, *Brevundimonas species* IITISM22 was found to have an impressive affinity towards the detoxification of Hg when used as a biosorbent in an aqueous medium¹⁴. Also, living microorganisms that produce extracellular polymeric substances (EPS) are believed to play an important role in metal biosorption¹⁵.

The immobilization of microbial cells on numerous matrices via entrapment was found to enhance bioremediation of heavy metals¹⁶ and dyes¹⁷ from wastewater. Immobilized microbial cells have following advantages over the free cells in metals biosorption process: easy manipulation, higher stability of composites, easy separation after biosorption procedures, potential use in real continuous systems¹⁸. Several matrices have been employed in immobilization of the biosorbents for heavy metal removal in order to improve biosorption. Entrapment of biosorbents in the alginate has been used for heavy metal removal, due to its easy preparation, biodegradability and hydrophilicity⁸. The major

advantage of alginate as a carrier is that immobilized cells do not undergo extreme changes in their physicochemical properties during immobilization procedure¹⁹. However, alginate cannot be maintained for a long time in aqueous medium, so the resulting alginate–microbial cell composite can easily be damaged during the water treatment²⁰.

However, the use of inorganic material such as silica as a carrier offers thermostability, non-toxicity, good mechanical strength, water stability (non-swelling), resistance to microbial degradation, as well as efficient sorption of metal ions²¹. Furthermore, mesoporous silica shows good adsorption capacity because of its high surface area, good selectivity and higher mass transport rates inside the porous structure¹⁹. Therefore, silica, as an inert material, which may act as a protector of immobilized cells, can be used as a suitable carrier for immobilization of biomass²².

Additional reasons for application of mesoporous silica for the removal of heavy metals from water sources are its tunable pore size and richness in hydroxyl groups which allows the functionalization by grafting reactions of the silanol groups on the surface of silica particles with organic silanes²³. Surface multi-functionality of these materials allows them to easily react chemically and bind/adsorb a specific target metal ion(s) on their surfaces. Amino-functionalized mesoporous silica materials (NH₂-SBA-15) prepared by post-grafting can be further functionalized by the formation of Schiff base between amine end-capped silica and polyvinylpyrrolidone (PVP) moieties²⁴. As a result, the NH₂-SBA-15 can display a moderate affinity toward heavy element ions under study. However, grafting of PVP moieties introduces a high affinity toward heavy metal ions²⁴.

Silica particles applied as a support of hydrophilic nanoparticles (HNP) have also been used for removal of cadmium ions from water^{25,26}. It was shown that the use of silica as support enhances the utilization range of the HNP active phase, making it more stable in a wider range of pH values. This was related to a stabilization of the solution pH due to the silica, which helps operating the HNPs in better conditions than those available when the particles are used in their colloidal form^{25,26}.

Silicates, mainly in the form of aqueous alkaline sodium silicate solutions (water glass) were used for the synthesis of silica prior to silicon alkoxides. Silicates are non-toxic aqueous precursors with low environmental impact and they can be used under solvent-free conditions²⁷. These properties of silicates allowed silicate-based processes to be recently re-investigated in the context of green sol–gel chemistry. It has been found that sodium silicates can be prepared by the fusion of silica sand with soda ash (sodium carbonate) or sodium hydroxide at 1100–1200 °C, with the resulting molten salt then being dissolved into water. During this process, it is possible to vary the Na:Si ratio in order to manipulate the nature of silicate types in the solution. Alternatively, silica can be extracted from higher plants, in particular, from *Gramineae* that transforms silicic acid into SiO₂, which is accumulated up to 20 wt%²⁸. Silica can also be extracted from rice hull ash using 1 mol/L NaOH. This extract was concentrated by volume reduction and adjusted to 3 mol/L NaOH. Concentrated silica extracts in 3 mol/L NaOH solution were used to produce flexible silicate films²⁹.

Having all this in mind, in order to make advanced biosorbents for removal of cadmium ions from aqueous solutions, we have developed two processing methods for immobilization of non-pathogenic and safe *Leuconostoc mesenteroides* and *Saccharomyces cerevisiae* cells. In the first method, microbial biomass was encapsulated by silica gel, whereas the second method was used for encapsulation of microbial biomass in silica-alginate composite material.

2. Materials and Methods

2.1. Cultivation of microbial biomass

The strain *Saccharomyces cerevisiae* (ATCC 2601) was maintained by subculturing on a Sabouraud Dextrose agar (SDA) (Merck) at 4 °C. The biomass of *S. cerevisiae* (ATCC 2601) was obtained by inoculation of SDA plates and incubation at 25°C for 48h. Culture suspension was prepared by carefully scraping (by sterile swab) in sterile distilled water and then centrifuged at 5000 rpm for 10 min, in order to separate the liquid (water) and solid (yeast biomass) phase. The yeast biomass was dried at 25°C for 12h, and grounded into fine particles. *Leuconostoc mesenteroides* (Institute of Molecular Biology and Genetical Engineering, Belgrade) was maintained by subculturing on MRS broth (Torlak, Serbia) at 4 °C. The 250 mL Erlenmeyer flask with MRS broth was used for bacteria growth at 32°C for 24h. The bacterial biomass was separated from the growth medium by centrifugation (6000 rpm for 10 min) and washed with sterile distilled water.

2.2. Effect of cadmium ions on viability of *L. mesenteroides* and *S. cerevisiae* cells

The preliminary examination of potential effects of different concentrations of cadmium solution on viability of *L. mesenteroides* and *S. cerevisiae* was performed by modified disc diffusion method³⁰. Briefly, the agar surfaces of MRS and SDA plates were inoculated with microbial suspension (inoculum 10⁶ cells/mL). Sterile filter paper discs (diameter 6 mm) (blank; HiMedia, Mumbai, India) were placed on the previously inoculated agar surfaces of the plates (Figure 1). Different concentrations of sterile cadmium solution (0.5, 1, 2, 4, 8 and 10 mM) were prepared and 15, 20, and 25 µL of cadmium solution for each concentration was individually added onto the sterile filter paper discs (Figure 1). The control samples were prepared by the same procedure, but instead of cadmium solution, the sterile water was added onto the sterile filter paper discs. Inoculated plates were incubated at 32°C for 48 hour (*L. mesenteroides*) and 25°C for 72 hours (*S. cerevisiae*) and the inhibition zone diameters were measured and expressed in millimeters. All experiments were performed in three replications. MS Excel (Microsoft Corporation, Redmond, WA) was used to calculate the mean and standard deviation.

2.3. Immobilization of *L. mesenteroides* and *S. cerevisiae* cells

Immobilization of *L. mesenteroides* and *S. Cerevisiae* cells was performed by two processing methods. In the first case, 0.564 g of *L. mesenteroides* or *S. Cerevisiae* cells

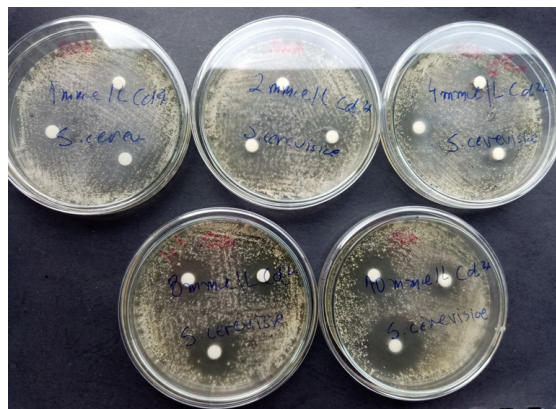


Figure 1. Determination of the effect of cadmium ions (cadmium concentration of 1, 2, 4, 8 and 10 mmol/L) on viability of *S. cerevisiae* cells.

were dispersed in 15 ml of silicate solution having a Na₂O/SiO₂ molar ratio of 0.4 and SiO₂ concentration 75.4 g/L, respectively (Figure 2a). The sulfuric acid (1 mol/L) was slowly added into stirred dispersion of cells and sodium silicate at 40°C to induce the generation (Figure 2b) and aggregation of silica nanoparticles, allowing the entrapment of yeast cells within the silica gel material (Figure 2c). The obtained silica-microbial cell material was washed, dried at room temperature and finally grinded into fine particles. The obtained samples were marked as S-Lm and S-Sc (Table 1).

In the second case, 0.375 g of the cell biomass was mixed with 2 ml of silicate solution (previously obtained by passing sodium silicate solution having a Na₂O/SiO₂ molar ratio of 0.4 and SiO₂ concentration 362 g/L, in cation-exchange resin (Amberlite IRC120 H, Supelco) and 8 ml of 5% w/v alginate solution. The mixture of sodium silicate, alginate and microbial cell was slowly added (Figure 3b) into previously prepared 0.1 M calcium chloride solution (Figure 3a). The silica-alginate/microbial cell material was washed and dried at room temperature. The obtained samples were marked as SA-Lm and SA-Sc (Table 1).

2.4. Removal of cadmium ions from aqueous solution

In order to test the cadmium ions removal ability of the free microbial cells and synthesized microbial based sorbents, as well as pure silica and pure alginate, a set of adsorption experiments was carried out. To investigate adsorption of cadmium ions from aqueous solution by *L. mesenteroides* or *S. cerevisiae* cells, 0.05 g of cell biomass was dispersed in 10 mL of 1 mmol/L aqueous cadmium(II) sulphate solution (pH = 6) under magnetic stirring. To investigate the adsorption of cadmium ions from aqueous solution by silica-microbial cell composites (samples S-Lm and S-Sc), 0.05 g of this composite material was dispersed in 10 mL of 1 mmol/L aqueous cadmium(II) sulphate solution. The adsorption of cadmium ions from aqueous solution by alginate-silica-microbial cell composites was investigated by dispersing of 0.2 g of this composite material in 10 mL of 1 mmol/L aqueous cadmium(II) sulphate solution. After

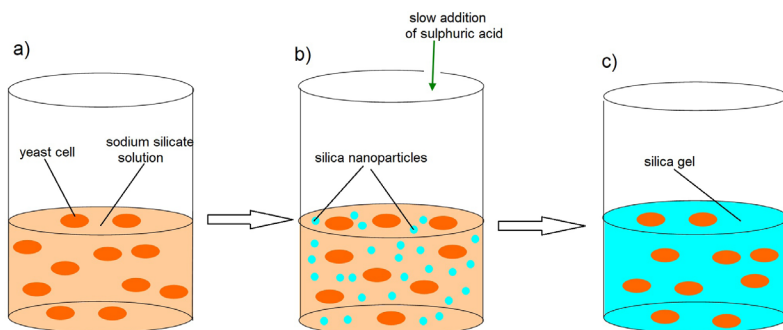


Figure 2. Preparation scheme of entrapment of microbial cells by silica gel.

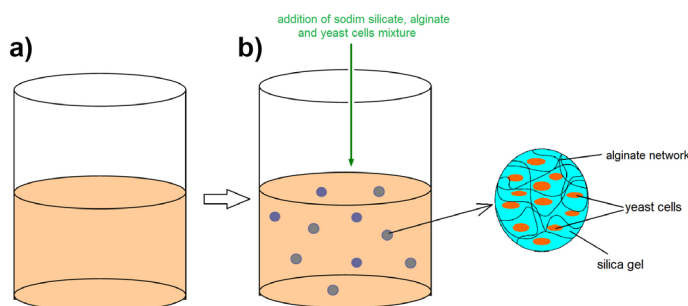


Figure 3. Preparation of alginate-silica-microbial cell composite materials.

Table 1. Experimental sample information.

Sample notation	Type of microorganism	Type of support	The support/ microorganism weight ratio	The mass of used composite for Cd removal (g/L)
S-Lm	<i>Leuconostoc mesenteroides</i>	Silica	2:1	5
S-Sc	<i>Saccharomyces cerevisiae</i>	Silica	2:1	5
SA-Lm	<i>Leuconostoc mesenteroides</i>	Silica-alginate	4:1	20
SA-Sc	<i>Saccharomyces cerevisiae</i>	Silica-alginate	4:1	20

appropriate contact time, the samples were centrifuged and small aliquots of supernatant were diluted in 1% (w/w) nitric acid. The effect of contact time was studied by varying time from 2 to 1400 minutes. The effect of pH value on cadmium removal by viable and immobilized cells was investigated at pH values 2, 4, 6 and 7. The effect of temperature on the removal of cadmium ions by the free microbial cells, pure alginate, pure silica material, as well as alginate-silica-microbial cells composite was also investigated. The influence of temperature was investigated at an initial sorbate concentration of 1 mmol/L and the temperature was varied from 15, 30, 40 to 50°C, respectively.

The cadmium concentration, both in the initial and final solution, was determined by flame atomic absorption spectrometry using Perkin Elmer AAnalyst 200 system after calibration with stock solutions in the range of concentration of 0.5–4 mg/L. The equilibrium amount (adsorption capacity)

(q_e) of cadmium ions adsorbed on sorbent phase (mg Cd²⁺/g dry sorbent) was calculated in the following way:

$$q_e = \frac{(C_0 - C_e) \cdot V}{m}$$

where C_0 (mg·L⁻¹) is the initial concentration of Cd²⁺, C_e (mg·L⁻¹) is the equilibrium concentration of Cd²⁺, V (L) is the total volume of solution and m (g) is the mass of adsorbent. All experiments were performed in triplicates and the mean values were used in the data analysis.

Equilibrium isotherms study of cadmium removal were performed at different concentrations of cadmium (0.5, 1, 2, 4, 8, 15, 30 mmol/L) and agitated for 3 h in a shaker at 30°C. The Langmuir adsorption model was utilized to describe and evaluate the experimental data³¹:

$$\frac{C_e}{q_e} = \frac{1}{q_m} C_e + \frac{1}{q_m b}$$

where, q_e was the equilibrium adsorption capacity of Cd^{2+} (mg/g), the q_m was the theoretical maximum adsorption capacity of Cd^{2+} (mg/g), C_e was the Cd^{2+} equilibrium concentration (mg/L) and b was the Langmuir constant (L/mg).

The effect of simultaneous action of interfering ions (Na^+ , Ca^{2+} , Mg^{2+} , Fe^{3+} , Zn^{2+} , Mn^{2+} , Cu^{2+} , CO_3^{2-} , Cl^- , SO_4^{2-}) on Cd^{2+} adsorption by silica-alginate-*L. mesenteroides* composite was investigated at 1 and 4 mmol Cd^{2+} , respectively. The concentration of each interfering ion was 20 mg/L.

2.5. Leaching studies of microbial cell/support composite particles

The leaching of microbial cells from prepared composites was examined during 5 cycles of incubation in sterile distilled water (for 90 min for every cycle) under magnetic stirring. 0.05 g of samples S-Lm and S-Sc were dispersed in 10 ml of sterile distilled water, respectively. On the other hand, 0.2 g of SA-Lm and SA-Sc were dispersed in 10 ml of sterile distilled water, respectively. After each cycle, supernatant was collected and aliquot of supernatant was put in a Petri plate that contains a growth medium. Microbial desorption experiments were conducted by controlling the viability of the yeast and bacteria after every agitation cycle using the agar plate count method. Bacteria were grown under aerobic conditions, at 32 °C for 12h in MRS agar (Torlak, Serbia). Incubation of the yeast was performed at 25 °C in SDA agar for 48h. All experiments were performed in three replications. MS Excel (Microsoft Corporation, Redmond, WA) was used to calculate the mean and standard deviation.

2.6. Characterization of materials

The size and morphology of the particles were examined using a scanning electron microscope (SEM, JSM-6390 LV JEOL, operating at 30 kV) coupled with EDS (Oxford Instruments X-MaxN). Prior to SEM imaging, the samples were sputtered with gold. The zeta potential of particles was measured by dynamic light scattering (Zetasizer Nano ZS, Malvern Instruments). IR spectra were recorded on

a Thermo Scientific Nicolet Summit FT-IR spectrometer, using the attenuated total reflectance (ATR) technique with diamond crystal (Smart Orbit, Thermo Scientific, Madison, WI, USA). Spectral data were collected in the mid-IR range (4000–400 cm^{-1}) with 32 scans and 4 cm^{-1} resolutions. Prior to recording of each sample's spectrum, the background spectrum (16 scans) was recorded before every sample spectrum.

3. Results and Discussion

3.1. The characterization of microbial cells

SEM micrographs of *Saccharomyces cerevisiae* and *Leuconostoc mesenteroides* cells are shown in Figure 4. Average diameter of the single *S. cerevisiae* and *L. mesenteroides* cell was about 5 and 0.5 μm , respectively. Aqueous electrophoresis curves of *L. mesenteroides* and *S. cerevisiae* cells are shown in Figure 5. Both cells exhibit negative surface charges at the investigated pH range between 2 and 10, which may enhance the adsorption of the positively charged metal ions through electrostatic forces.

EDS analysis with chemical mapping of *S. cerevisiae* (a) and *L. mesenteroides* (b) after exposure to Cd^{2+} ions from aqueous solution is shown in Figure 6. The chemical mapping showed that the blue spots correspond to the cadmium ions bound by cell. The presence of phosphorous on *L. mesenteroides* cells might be the consequence of its cultivation onto MRS broth containing dipotassium phosphate.

The adsorption isotherms of *L. mesenteroides* and *S. cerevisiae* cells are shown in Figure 7. Maximum adsorption capacity of *S. cerevisiae* and *L. mesenteroides* cells was 18.5 and 78 mg/g, respectively. Comparative study of zinc binding capacity by three lactic acid bacteria (LAB) was examined by Mrvčić et al.³². The most effective LAB was *L. mesenteroides* (27.10 mg Zn^{2+} /g biomass). Yi et al.³³ were studied potential use of *L. mesenteroides* for the removal of Pb(II) ions. The *L. mesenteroides* sp. showed greater lead resistance and removal capacity (the maximum adsorption capacity of this strain was 60.6 mg Pb/g). Although, results obtained by these authors suggest that the adsorption was mainly mediated by exopolysaccharides³³.

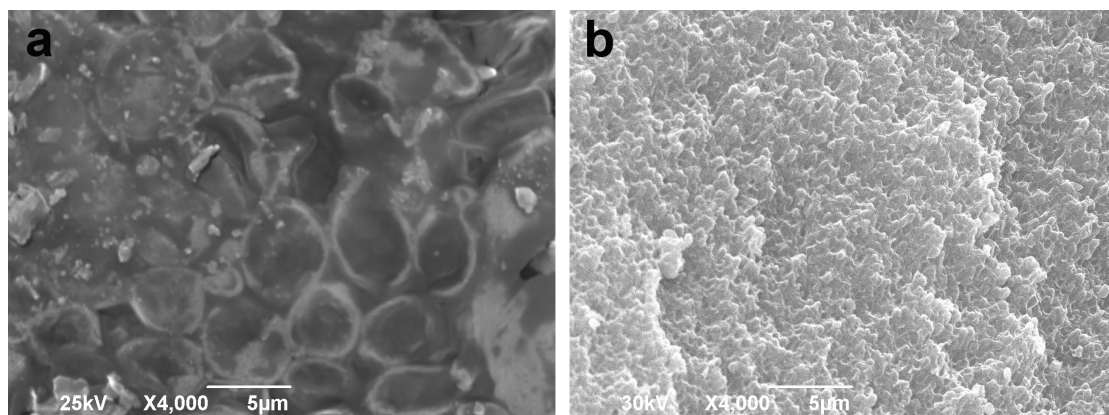


Figure 4. SEM micrographs of *Saccharomyces cerevisiae* (a) and *Leuconostoc mesenteroides* (b) cells.

3.2. Effect of different concentration of cadmium solutions on viability of *L. mesenteroides* and *S. cerevisiae*

The results of the effects of cadmium on viability of *L. mesenteroides* and *S. cerevisiae* obtained by disk diffusion method are given in Table 2 (The results are also presented in Figure 1). The results showed inhibitory effect of cadmium ions for both microorganisms at cadmium concentration higher than 2 mM. The inhibition zones for *S. cerevisiae* were larger than those for *L. mesenteroides*, indicating that *L. mesenteroides* exhibits greater resistance. Furthermore, the cadmium concentrations of 0.5, 1 and 2 mM had no effect on viability of both *L. mesenteroides* and *S. cerevisiae*. The higher resistance to stress caused by cadmium, as well as the higher adsorption capacity of *L. mesenteroides* cells relative to that of *S. cerevisiae* cells, might be attributed to extra cellular production of dextran by *L. mesenteroides* cells that are believed to play an important role in metal biosorption by microorganisms³⁴.

FTIR spectra of micelles obtained after incubation of *L. mesenteroides* in distilled water and 1 mmol/L aqueous cadmium(II) sulphate solution for 24 hours, under magnetic

stirring, is shown in Figure 8, respectively. Intense absorption band in the region at 3360 cm^{-1} can be assigned to the stretching vibration of hydroxyl group bounds, indicating the presence of a polyhydroxilic compound. The band in the region at 2928 cm^{-1} is due to stretching vibrations of C-H bonds.

The band in the region at 1636 cm^{-1} was due to bound water³⁵. The main absorption bands that characterize the dextran α -(1 \rightarrow 6) exopolysaccharide were found in the region of 1152 cm^{-1} , being related to the vibrations of glycoside C-O-C bonds, as well as at 912 cm^{-1} and indicating the existence of this glycoside bond in the alpha (α) conformation³³. The weak peak at 866 cm^{-1} was characterized as α -D-glucose. The FTIR spectra clearly show the presence of dextran produced by *L. mesenteroides*. However, more intense bands were obtained in the presence of cadmium

Table 2. Cadmium effect on viability of *L. mesenteroides* and *S. Cerevisiae*.

Cadmium concentration (mM)	Amount (μL)	Diameter of inhibition zone (mm) (mean \pm SD*)	
		<i>Leuconostoc mesenteroides</i>	<i>Saccharomyces cerevisiae</i>
0.5	15	-	-
	20	-	-
	25	-	-
1	15	-	-
	20	-	-
	25	-	-
2	15	-	-
	20	-	-
	25	-	-
4	15	8.3 \pm 0.57	12.0 \pm 0.00
	20	11.0 \pm 0.00	17.3 \pm 0.57
	25	12.0 \pm 0.00	20.6 \pm 1.15
8	15	10.3 \pm 0.57	15.0 \pm 0.00
	20	12.0 \pm 0.00	20.6 \pm 1.15
	25	14.6 \pm 1.15	23.0 \pm 0.00
10	15	12.0 \pm 0.00	18.6 \pm 1.15
	20	14.0 \pm 1.00	23.0 \pm 0.00
	25	18.0 \pm 0.00	29.3 \pm 0.57

*standard deviation

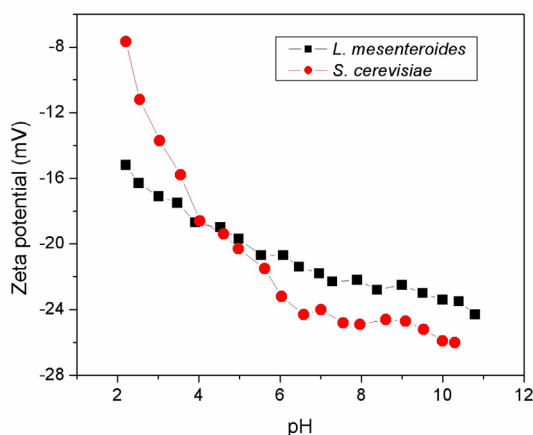


Figure 5. Aqueous electrophoresis curves obtained for *L. mecenteroides* and *S. cerevisiae* cells.

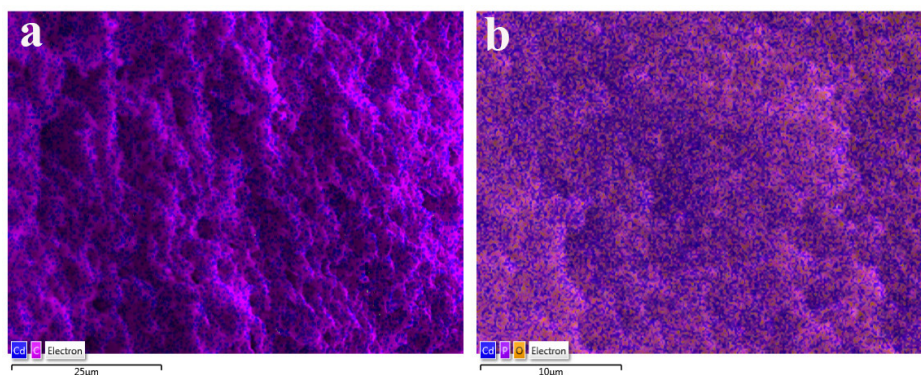


Figure 6. EDS spectrum and chemical mapping of the *S. cerevisiae* (a) and *L. mesenteroides* (b) cells after exposure to Cd^{2+} ions.

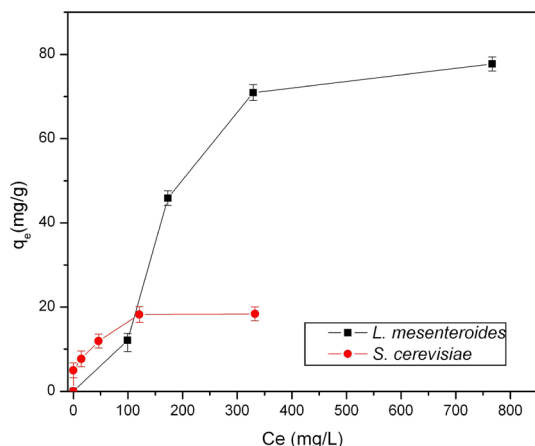


Figure 7. Adsorption isotherms for *S. cerevisiae* and *L. mesenteroides* cells obtained at 30°C.

ions, indicating the fact that cadmium ions not only induce bacterial exopolysaccharides synthesis in response to heavy metal stress, but also the produced exopolysaccharides which can appreciably adsorb this metal³⁴.

3.3. Entrapment of microbial cells by silica gel

SEM micrograph of composite particles obtained by entrapment of *S. cerevisiae* and *L. mesenteroides* cells by silica gel are shown in Figure 9a (sample S-Sc) and 9b (sample S-Lm), respectively. Obtained particles are polydispersed with irregular shape. The separate microbial cells are also visible, indicating the release of cells after grinding in fine particles.

The results of the microbial cell leaching from the silica support during stirring in sterile water are shown in Table 3. The greatest leaching of the yeast cells from silica/yeast composite particles (sample S-Sc) was noticed after the first cycle and was 80 CFU/ml. Leaching process gradually decreased over the next three cycles and was 31, 21 and 10 CFU/ml, respectively.

The leaching of yeast cells was not detected after the 5th cycle. On the other hand, bacteria cell leaching from silica/*L. mesenteroides* composite was 90 CFU/mL after the first and the second cycle, respectively. Then it grew on 102.6, 161.3 and 1201.6 CFU/mL, after the third, fourth and fifth cycle, respectively.

Based on these results, it can be concluded that desorption of bacteria cells from silica carriers is more intense than yeast cells, probably due to smaller cell dimensions of *L. mesenteroides* cells allowing the faster leaching of bacterial cells.

The adsorption capacity of cadmium ions by *L. mesenteroides*/silica and *S. cerevisiae*/silica composite particles is shown in the Figure 10. The saturation capacity of *L. mesenteroides*/silica composite particles of ~40.75 mg/g was reached after three cycles (Figure 10a). The saturation capacity of *S. cerevisiae*/silica composite particles of ~26.71 mg/g was reached after two cycles (Figure 10b). These results show the higher binding capacity of *L. mesenteroides*/silica composite particles which is in correlation with previous results that showed higher binding

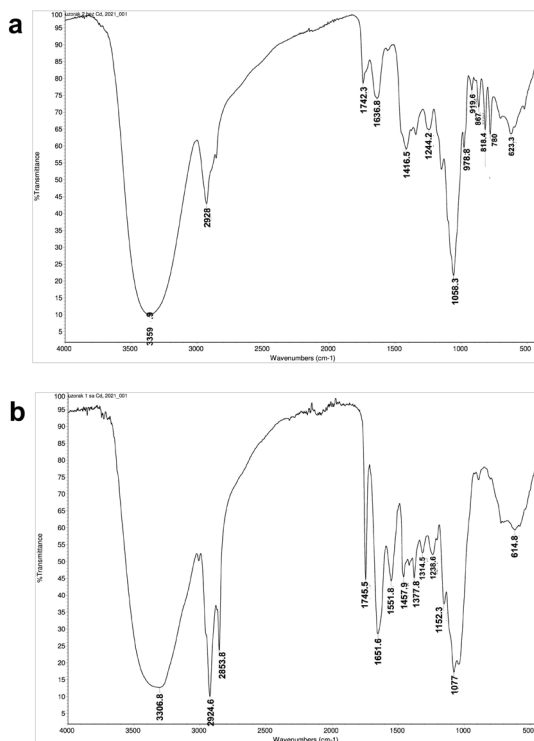


Figure 8. FT-IR spectrum of exopolysaccharides produced from *L. mesenteroides*: a) 24 hours of incubation in aqueous solution; b) 24 hours of incubation in 1 mmol/L aqueous cadmium(II) sulphate solution.

capacity of free *L. mesenteroides* cells relative to *S. cerevisiae* cells. Compared to free microbial cells, the same weight of the silica/microbial cell composite (the silica/microbial weight ratio was 2:1) displayed higher binding capacity, indicating the important contribution of silica in adsorption of cadmium ions.

3.4. Entrapment of microbial cells by silica-alginate composite particles

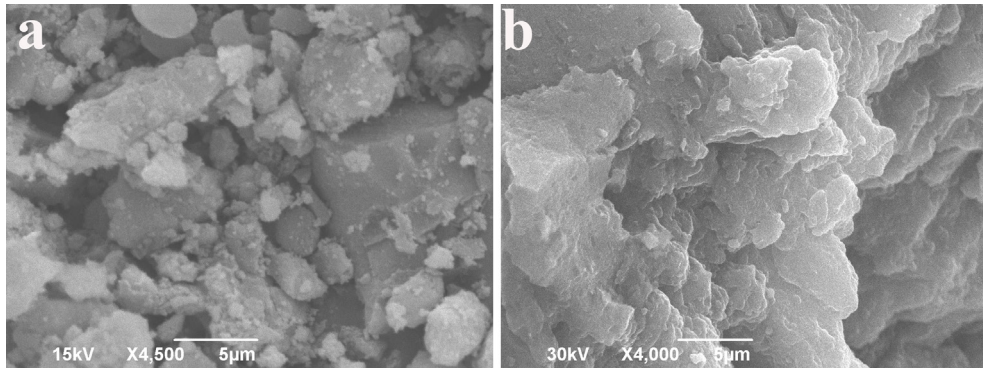
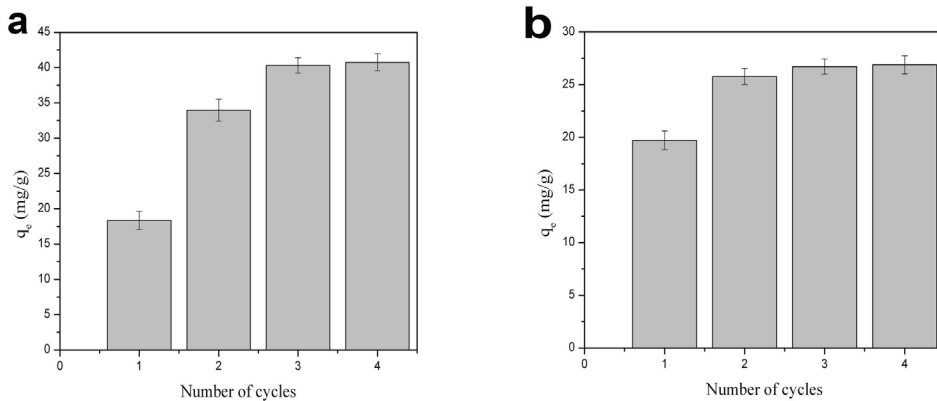
To overcome the problems arising from the use of powdered microbial cell/silica composites (e.g. separation of composite particles from mixture, leaching of cells from composites), the new approach of microbial cell entrapment was developed. This approach was based on dispersion of microbial cells in silicate/alginate solution followed by a dropwise addition into CaCl_2 solution in order to induce gelling of alginate and formation of spherical particles.

Figure 11 shows SEM micrographs of silica-alginate-*S. cerevisiae* (a, b) and silica-alginate-*L. mesenteroides* (c, d) composite particles. Average particle size is about 1.5 μm . The microbial cells are clearly visible on the surface of particles. In order to visualize the internal structure of the composite particle, a SEM characterization with EDS mapping of the cross sectional area of silica-alginate-*S. cerevisiae* and silica-alginate-*L. mesenteroides* composites (used in 12 adsorption cycles of cadmium from aqueous solution) was also performed (Figure 12). EDS maps (Figure 12b and 12e) clearly show the dispersion of cadmium (blew spots), silicon (green spots) and calcium (violet spots), indicating that

Table 3. The leaching of microbial cell entrapped in silica gel.

Sample	Cell desorption (CFU/mL) (mean±SD*)				
	Cycles				
	1	2	3	4	5
S-Sc	80.0±1.15	31.0±1.53	21.0±1.00	10.00±0.00	-
S-Lm	90.0±0.00	90.3±0.57	102.6±2.51	161.3±1.15	1201.6±2.88

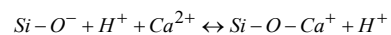
*standard deviation

**Figure 9.** SEM micrographs of silica-*S. cerevisiae* (a) and silica-*L. mesenteroides* (b) composite particles.**Figure 10.** The effect of adsorption cycle number on cadmium binding capacity of *L. mesenteroides*/silica (a) and *S. cerevisiae*/silica (b) composite particles.

the Cd is well dispersed in the cross-section of particles. The cavities with size of 200 μm (Figure 12 a, b) were also formed in the sample silica-alginate-*S. cerevisiae*, probably as a consequence of the shrinkage of silica gel during aging at ambient conditions. However, the cavities were not seen in the silica-alginate-*L. mesenteroides* sample, indicating that the dextran produced by *L. mesenteroides* acts as an efficient binder of silica nanoparticles³⁶ preventing the shrinkage of silica gel during aging. EDS mapping image (Figure 12e) also shows that calcium is mainly distributed on the surface of the silica-alginate-microbial composite particles, indicating the formation of calcium alginate outer surface layer.

Different interactions may occur between components of the silica-alginate-microbial cell composite. On the surface of silica nanoparticles there are many silanol groups, which

can be deprotonated³⁷. Ca^{2+} ions, derived from a salt, can react with deprotonated silanol group³⁸:



The positively charged obtained silica surface can adsorb negatively charged alginate groups. The surface of *L. mesenteroides* cell is also covered with a thin layer of dextrane³⁹. Dextran functional hydroxyl groups also offer an easy point for chemical conjunction with alginate and silica. As a result of all these interactions, the formation of stable composite material is allowed.

The Energy Dispersive X-ray analysis (chemical mapping and energy spectrum) of external (a) and internal (b) surface of silica-alginate-*S. cerevisiae* (sample SA-Sc) and

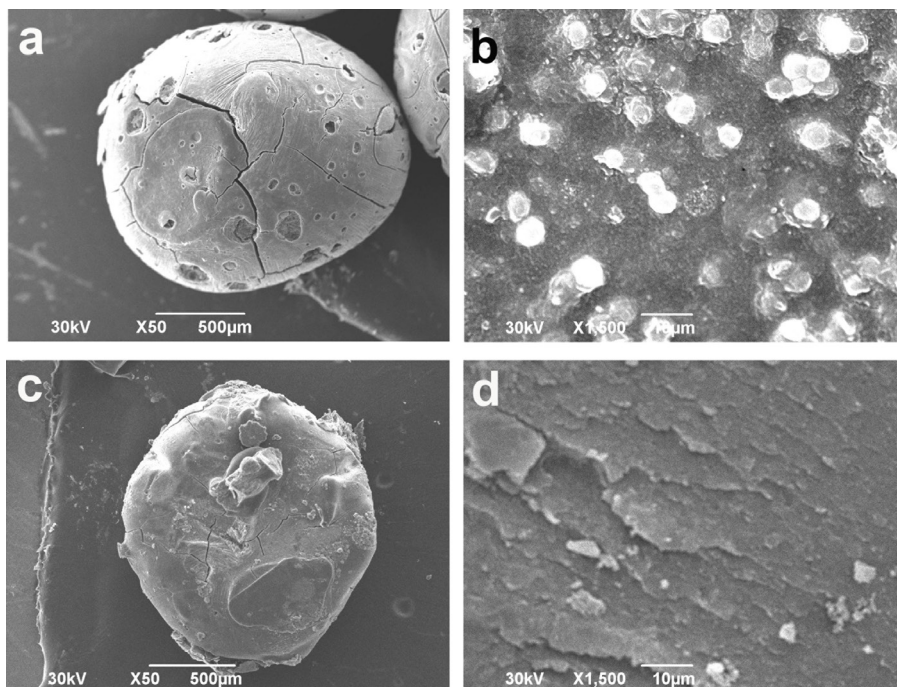


Figure 11. SEM micrographs of silica-alginate-*S. cerevisiae* (a, b) and silica-alginate-*L. mesenteroides* (c, d) composite particles.

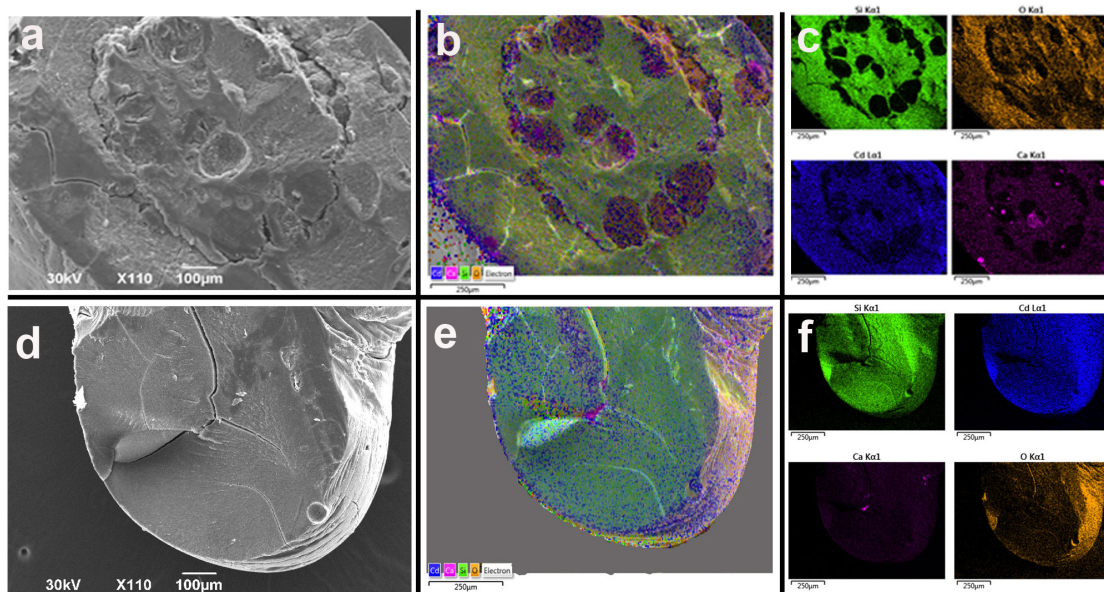


Figure 12. SEM micrograph and EDS mapping images of the cross sectional area of silica-alginate-*S. cerevisiae* (a, b, c) and silica-alginate-*L. mesenteroides* (d, e, f) composites used for 12 adsorption cycles of cadmium from aqueous solution.

silica-alginate-*L. mesenteroides* (sample SA-Lm) composites used in 12 adsorption cycles of cadmium from aqueous solution are shown in Figure 13 and Figure 14, respectively. EDS analysis of the external surface shows the presence of high levels of cadmium (27.24 wt. %) accumulated during 12 adsorption cycles (Figure 13a). On the other hand, the cadmium content in internal area was slightly lower (11.39 wt. %) (Figure 13b), indicating the diffusion limitation of cadmium ions through

the porous structure of silica-alginate-*S. cerevisiae* composite. The level of cadmium on the external and internal surface of silica-alginate-*L. mesenteroides* (sample SA-Lm) was 13.71 and 12.5 wt.%, respectively, indicating that the lower mass transfer resistance is probably caused by different silica porosity due to dextran action.

The results of the leaching of microbial cells from silica-alginate support during stirring in sterile water are

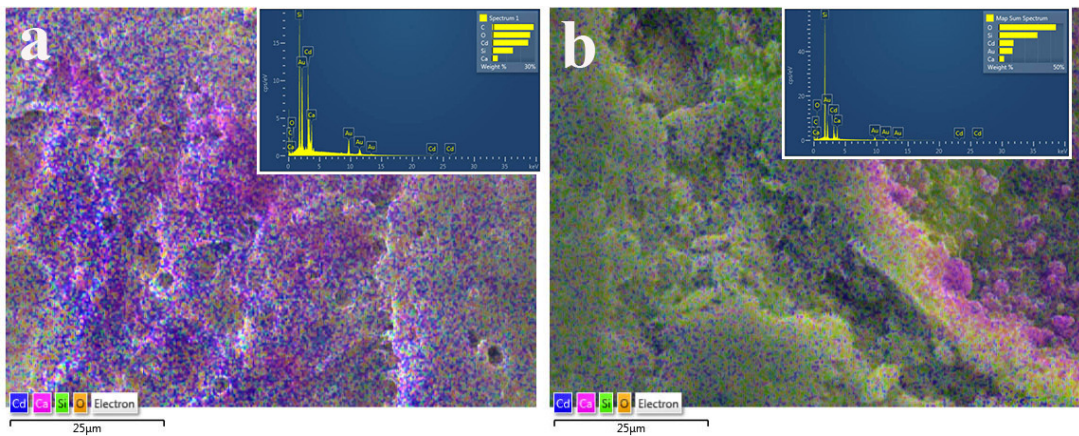


Figure 13. EDS analysis of the external (a) and internal (b) surface of silica-alginate-*S. cerevisiae* composite (sample SA-Sc).

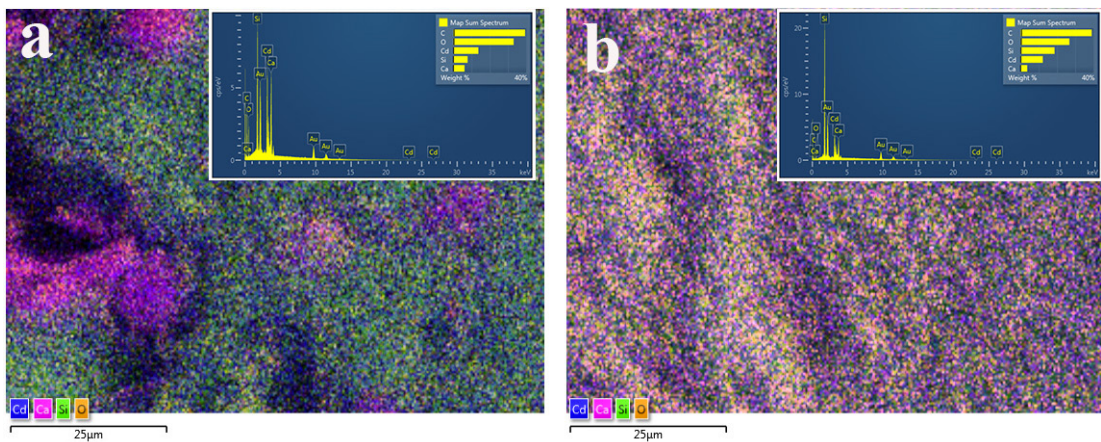


Figure 14. EDS analysis of the external (a) and internal (b) surface of silica-alginate-*L. mesenteroides* composite (sample SA-Lm).

Table 4. The leaching of microbial cell entrapped in silica-alginate composite particles.

Sample	Cell desorption (CFU/mL)(mean±SD*)				
	Cycles				
	1	2	3	4	5
SA-Sc	10.33±0.577	-	-	-	-
SA-Lm	20.66±1.154	10.0±0.00	-	-	-

*standard deviation

shown in the Table 4. The leaching of yeast cells from silica/yeast composite particles (sample SA-Sc) after the first cycle was only 10.33 CFU/ml. In the next four cycles, no leaching was detected. On the other hand, the leaching of bacteria cells was 20.66 and 10 CFU/ml after the first and the second cycle, respectively. In the next three cycles, no leaching was detected. The leaching of bacteria cells was higher relative to the leaching of the yeast cells probably due to their smaller size which allows easier leaching from the surface of support. However, the leaching of microbial cells from the alginate-silica composite particles was much lesser than the leaching from the silica powder (samples S-Sc and S-Lm) indicating that the second entrapment method could be useful for leaching prevention.

3.5. The effect of pH, temperature and time on binding capacity of microbial biomass-silica-alginate biosorbent

The effect of pH on relative adsorption capacity of *L. mesenteroides* and *S. cerevisiae*, as well as, SA-Lm and SA-Sc composites is shown in the Figure 15. The relative adsorption capacity of the free cells was also shown and increased with increasing pH. The reason for this is the change in the cells zeta potential which became more negative as the pH of the solution increased (Figure 5). This effect promotes the adsorption of positive cadmium ions. The immobilized cells show a broader pH activity profile compared to the free cells. The immobilized cells

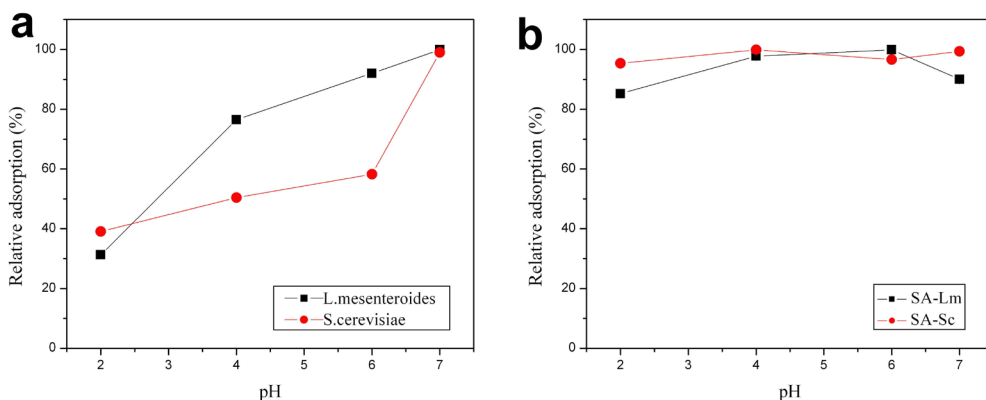


Figure 15. The effect of pH on binding capacity of microbial cells (a) and SA-Lm and SA-Sc composites (b).

possessed more than 80% relative adsorption capacity in the pH range 2.0–7.0. The higher adsorption capacities might be attributed to the multipoint attachment of cells to silica-alginate support, which buffered variability of cells when the pH was changed⁴⁰.

The effect of temperature on the removal of cadmium ions by pure silica, pure alginate, *L. mesenteroides*, *S. cerevisiae*, silica-alginate-*L. mesenteroides* and silica-alginate-*S. cerevisiae* composites is shown on Figure 16. The cadmium removal by *S. cerevisiae* cells increases with the increase of temperature. This showed that biosorption of heavy metals can be realized by different components of yeast cells, such as cell wall, cell membrane and cytoplasm³¹. It is obvious that an increase in temperature promotes diffusion of cadmium ions through cell wall and cell membrane and their accumulation in cytoplasm.

The surface of alginate based adsorbent is rich with functional groups including hydroxyl, carboxyl, amino, phosphonate and sulfonate groups. There was no significant change in binding capacity of alginate with temperature increase. This indicates that electrostatic forces rather than chemical bonds exist between functional groups of alginate and cadmium ions. *L. mesenteroides* cells displayed low relative binding capacity at 15°C (56.4%), and the highest relative binding capacity was reached at 30°C. At higher temperatures, 40 and 50°C, the relative binding capacity was about 82%. The highest extracellular dextran production by *L. mesenteroides* cells was obtained at 30°C⁴¹. The fact that both the highest binding capacity and the highest dextran production of *L. mesenteroides* were observed at the same temperature may indicate that dextran plays an important role in cadmium removal. The adsorption capacity of pure silica decreases with the temperature due to the exothermicity of the adsorption process²⁶. The relative binding capacity for the microbial-silica-alginate composites (samples SA-Lm and SA-Sc) is not significantly affected by temperature. The sample SA-Lm has slightly less relative binding capacity at 15°C, probably due to reduced dextran production at lower temperatures.

The effect of reaction time on cadmium binding capacity of SA-Lm and SA-Sc composite particles is shown in the Figure 17. The saturation capacity of samples was reached after approximately 180 minutes. The equilibrium amount

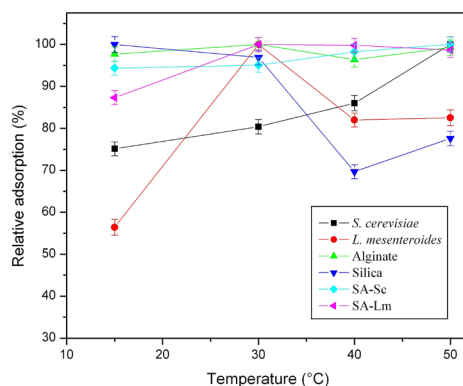


Figure 16. The effect of temperature on binding capacity of prepared adsorbent.

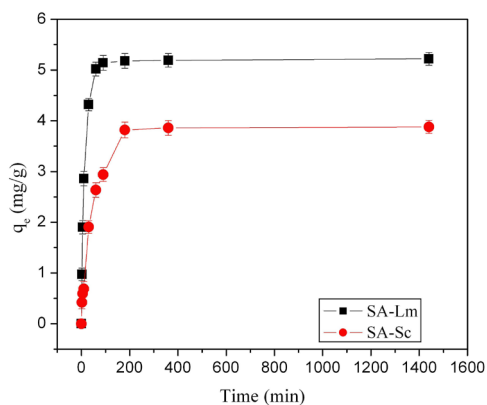


Figure 17. Effect of reaction time on cadmium binding capacity of SA-Lm (■) and SA-Sc (●) composites.

(adsorption capacity) (q_e) of cadmium ions adsorbed on SA-Lm and SA-Sc sorbent phase was 5.2 and 3.7 mg/g, respectively, indicating the higher binding capacity of silica-alginate composite with *L. mesenteroides* cells.

3.6. Biosorption isotherms of pure and composite materials

The effect of adsorption cycle number on cadmium binding capacity at pH=6 of *L. mesenteroides* and *S. cerevisiae* cells entrapped by silica-alginate composite particles (samples SA-Sc and SA-Lm) is shown on Figure 18. Saturation capacity of *L. mesenteroides* entrapped in silica-alginate composite particles was reached after 24 cycles and was about 93 mg/g. On the other hand, saturation capacity of *S. cerevisiae* entrapped in silica-alginate composite particles was reached after 12 cycles and was about 33 mg/g. These results indicate the higher binding capacity of *L. mesenteroides* cells entrapped in silica/alginate particles relative to *S. cerevisiae* cells. As it was discussed above, the higher adsorption capacity of immobilized *L. mesenteroides* cells might be

attributed to extracellular dextran production of bacterial cells. Compared to the powdered silica/*L. mesenteroides* cell composites (sample S-Lm), the saturation speed of silica-alginate-*L. mesenteroides* composite (the saturation capacity was reached after 24th cycle) was decreased due to the limited diffusion of the cadmium ions, which was caused by the internal mass transfer resistance. This resistance occurs in interstitial pores of larger silica-alginate-microbial cell composites and this problem could be solved by increasing the total pore size of composites.

Langmuir adsorption isotherms for free *S. cerevisiae* cells and synthesized microbial based sorbents (samples SA-Sc and SA-Lm) are shown in Figure 19. The curve-fitting parameters were summarized in Table 5. The affinity constant obtained from the Langmuir model was 0.07 for *S. cerevisiae*, 0.0066 for silica, 0.009 for alginate,

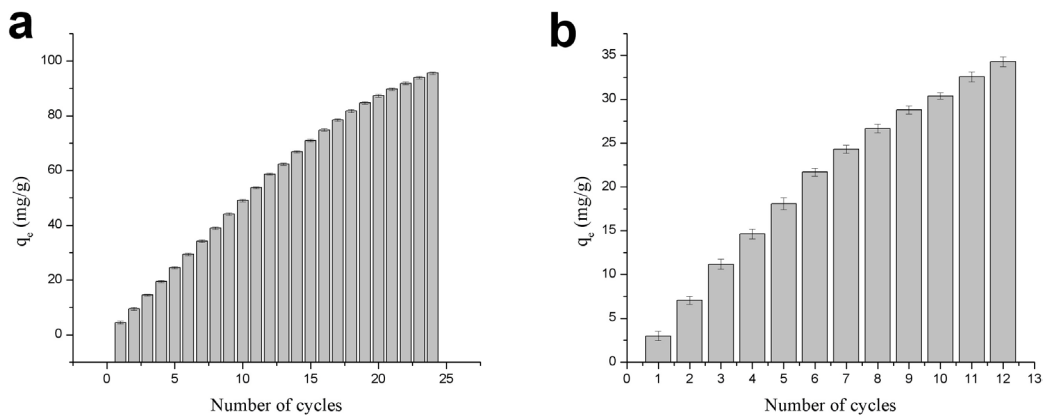


Figure 18. The effect of adsorption cycle number on cadmium binding capacity of silica-alginate-*L. mesenteroides* (a) and silica-alginate-*S. cerevisiae* composite particles (b).

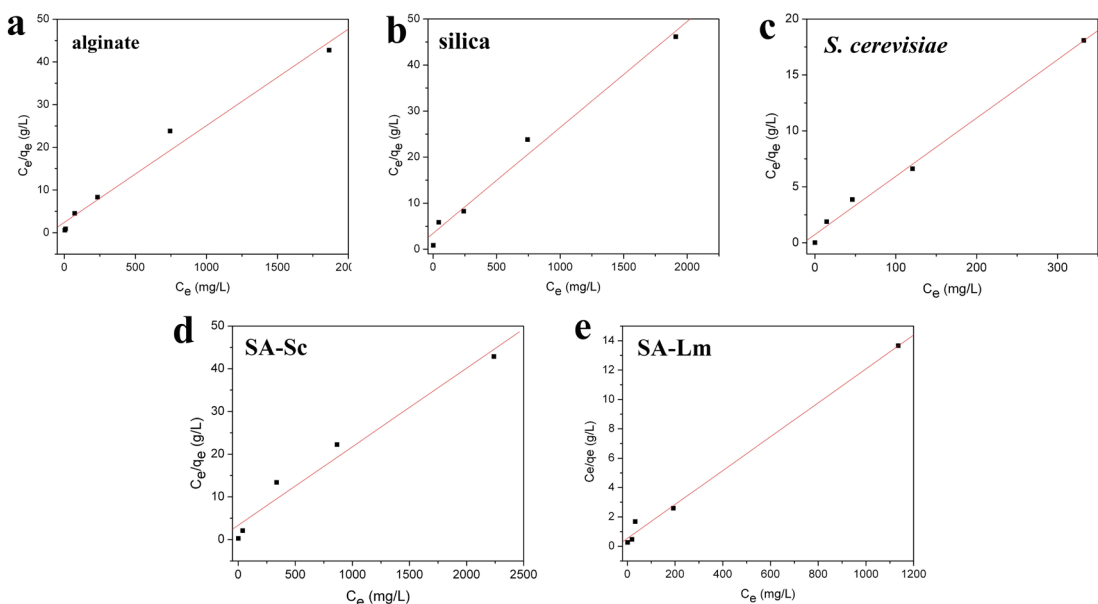


Figure 19. Langmuir adsorption isotherms for different adsorbents: a) alginate; b) silica; c) *S. cerevisiae*; d) silica-alginate-*S. cerevisiae* composite; e) silica-alginate-*L. mesenteroides* composite.

Table 5. Isotherm model parameters for adsorption of Cd²⁺ ions using Langmuir model.

Sample	<i>S. cerevisiae</i>	Silica	Alginate	SA-Lm	SA-Sc
q _m (mg/g)	19.2	43.59	44.24	86.65	54.377
b (L/mg)	0.07	0.0066	0.009	0.0213	0.00547
R ²	0.9932	0.9841	0.9774	0.9938	0.966

0.0213 for SA-Lm, and 0.00547 L/mg for SA-Sc (Table 5). Isotherm data for *L. mesenteroides* cells did not have a good fit with Langmuir model probably due to intensive production of dextrane that acts as a new biosorption site. However, as shown in Figure 7, this resulted in high value of the maximum binding capacity (78 mg/g). *S. cerevisiae* cells have a greater affinity for Cd²⁺ than silica or alginate. *S. cerevisiae* wall represents 30% of the dry weight of the cell and is composed largely of polysaccharides (85%) and proteins (15%)⁴². The maximum adsorption capacity of *S. cerevisiae* cells was 19.2 mg/g.

Silica-alginate-*L. mesenteroides* composite (sample SA-Lm) displays the greater affinity for Cd²⁺ (b=0.0213 L/mg) and greater binding capacity (86.65 mg/g) than other adsorbents. This can be explained by the action of dextrane produced by immobilized *L. mesenteroides* cells. Compared to the adsorption capacity of SA-Lm obtained after 24 cycles at initial Cd²⁺ concentration of 1 mmol/L (93 mg/g) (Figure 18a), the maximum binding capacity of SA-Lm obtained by the Langmuir model was slightly lower. The fact that the experimental data fits well with the Langmuir isotherm can be explained by the homogeneous distribution of active centers on SA-Lm and SA-Sc composites, since the Langmuir equation assumes that the surface is homogeneous⁴³.

3.7. Effect of interfering co-ions on cadmium removal

Industrial wastewater usually contains other co-ions that can interfere with treatment processes⁸. Table 6 shows the effect of simultaneous action of co-existing ions (Na⁺, Ca²⁺, Mg²⁺, Fe³⁺, Zn²⁺, Mn²⁺, Cu²⁺, CO₃²⁻, Cl⁻, SO₄²⁻) on Cd(II) adsorption onto silica-alginate-*L. mesenteroides* composite at initial cadmium concentrations of 1 and 4 mmol/L, respectively. Results demonstrated that Cd(II) removal performance was not significantly affected by the presence of these ions, suggesting that there was a large number of adsorption sites in silica-alginate-*L. mesenteroides* composite, which prevent the competitive action of co-ions present in wastewater. Furthermore, the removal efficiency at 4 mmol/L was higher probably due to more intense dextran secretion at higher cadmium concentrations.

Generally regarded as safe *S. cerevisiae* and *L. mesenteroides* cells have been widely involved in numerous fermentation processes and represent the sludge remaining as a residue at the bottom of fermentation tanks. The sodium silicate solution can be obtained from agricultural waste²⁹. On the other side sodium alginate can be obtained from renewable biomass⁴⁴ or by some bacterial species using the low cost carbon sources (molasses, maltose, and starch)⁴⁵. Having all this in mind, the obtained composite consisting of microbial biomass entrapped in silica-alginate composite particles can be recognized as a sustainable solution for wastewater treatment and belongs to the group of the low cost material⁴⁶.

Table 6. Effect of interfering ions on Cd²⁺ adsorption by SA-Lm composite. The initial Cd²⁺ concentration were 1 and 4 mmol/L, respectively, and the concentration of each interfering ion was 20 mg/L.

Initial Cd ²⁺ concentration	1 mmol/L	4 mmol/L
Removal efficiency (%)	92.77	99.27
Binding capacity (mg/g)	5.18	20.99

4. Conclusion

In this article, in order to produce advanced biosorbents for cadmium removal from aqueous solutions, two novel processing methods for immobilization of non-pathogenic and safe *Leuconostoc mesenteroides* and *Saccharomyces cerevisiae* cells have been presented. The first method is based on microbial biomass encapsulation by silica gel, whereas the second method was used for encapsulation of microbial biomass in silica-alginate composite material. The cadmium binding capacity of the *Leuconostoc mesenteroides* and *Saccharomyces cerevisiae* cells entrapped by the silica gel was ~40.75 and ~26.71 mg/g, respectively, indicating the contribution of the mesoporous silica to cadmium binding. It has been found that extracellular production of dextrane by *L. mesenteroides* cells might play an important role in metal biosorption by microorganisms. It was observed that the developed composite material displayed the leaching of microbial cells, with a higher degree of leaching for small size *Leuconostoc mesenteroides* cells. Furthermore, the entrapment of microbial cells in silica-alginate particles prevents desorption, resulting in high binding capacity of 93 mg/g for immobilized *Leuconostoc mesenteroides* cells and theoretical maximum binding capacity of 54 mg/g for immobilized *Saccharomyces cerevisiae* cells. Biosorption of Cd(II) by *Leuconostoc mesenteroides* entrapped in silica-alginate composite particles was not affected by the presence of Na⁺, Mg²⁺, Ca²⁺, Zn²⁺, Fe³⁺, Cu²⁺ and Mn²⁺ ions in studied concentrations, suggesting that there was a large number of adsorption sites in used composite. The obtained composite consisting of microbial biomass entrapped in silica-alginate composite particles can be recognized as a sustainable solution for wastewater treatment and belongs to the group of the low cost material.

5. Acknowledgments

This work was financially supported by the Ministry of Education, Science and Technological Development of the Republic of Serbia, project ref. number 451-03-9/2021-14 and project ref. number 451-03-68/2022-14. The authors would like to thank European Commission, Joint Research

Centre, Institute for Reference Materials and Measurements, for donation of Perkin Elmer AA200 flame atomic absorption spectrometer. The authors are also grateful to Institute of Molecular Genetics and Genetic Engineering (University of Belgrade) for generous gift of *Leuconostoc mesenteroides*.

6. References

- Hazrat A, Khan E, Ilahi I. Environmental chemistry and ecotoxicology of hazardous heavy metals: environmental persistence, toxicity, and bioaccumulation. *J Chem.* 2019;1-14.
- Genchi G, Stefania Sinicropi M, Lauria G, Carocci A, Catalano A. The effects of cadmium toxicity. *Int J Environ Res Public Health.* 2020;17:3782.
- Tinkov AA, Filippini T, Ajsuvakovae OP, Skalnaya MG, Aasethf J, Bjørklundh G, et al. Cadmium and atherosclerosis: a review of toxicological mechanisms and a meta-analysis of epidemiologic studies. *Environ Res.* 2018;162:240-60.
- IARC: International Agency for Research on Cancer. Monographs on the evaluation of the carcinogenic risks to humans beryllium, cadmium, mercury and exposures in the glass manufacturing industry. Lyon, France: IARC Scientific Publications; 1993. p. 119-238.
- Kubier A, Wilkin RT, Pichler T. Cadmium in soils and groundwater: a review. *Appl Geochem.* 2019;108:104388.
- Cheng X, Drozdova J, Danek T, Huang Q, Qi W, Yang S, et al. Pollution assessment of trace elements in agricultural soils around copper mining area. *Sustainability.* 2018;10:4533.
- He J, Chen JP. A comprehensive review on biosorption of heavy metals by algal biomass: Materials, performances, chemistry, and modeling simulation tools. *Bioresour Technol.* 2014;160:67-78.
- Aryal M. Calcium alginate entrapped *Eupatoriumadenophorum* Sprengel stems powder for chromium (VI) biosorption in aqueous mediums. *PLoS One.* 2019;14:e0213477.
- Mishra A, Gupta B, Kuma N, Singh R, Varma A, Thakur IS. Synthesis of calcite-based bio-composite biochar for enhanced biosorption and detoxification of chromium Cr (VI) by *Zhihengliuella* sp. *ISTPL4. Bioresour Technol.* 2020;307:123262.
- Khakpour H, Younesi H, Mohammadhosseini M. Two-stage biosorption of selenium from aqueous solution using dried biomass of the baker's yeast *Saccharomyces cerevisiae*. *J Environ Chem Eng.* 2014;2:532-42.
- Fomina M, Gadd GM. Biosorption: current perspectives on concept, definition and application. *Bioresour Technol.* 2014;160:3-14.
- Dhankhar R, Hooda A. Fungal biosorption – an alternative to meet the challenges of heavy metal pollution in aqueous solutions. *Environ Technol.* 2011;32:467-91.
- Pereira EJ, Ramaiah N. Chromate detoxification potential of *Staphylococcus* sp. isolates from an estuary. *Ecotoxicology.* 2019;28:457-66.
- Singh S, Kumar V, Gupta P, Ray M, Kumar A. The synergy of mercury biosorption through *Brevundimonas* sp. IITISM22: Kinetics, isotherm, and thermodynamic modeling. *J Hazard Mater.* 2021;415:125653.
- Li W-W, Yu H-Q. Insight into the roles of microbial extracellular polymer substances in metal biosorption. *Bioresour Technol.* 2014;160:15-23.
- Keskin NOS, Celebioglu A, Sarioglu OF, Uyar T, Tekinay T. Encapsulation of living bacteria in electrospun cyclodextrin ultrathin fibers for bioremediation of heavy metals and reactive dye from wastewater. *Colloids Surf B Biointerfaces.* 2018;161:169-76.
- San NO, Celebioglu A, Tümtaş Y, Uyar T, Tekinay T. Reusable bacteria immobilized electrospun nanofibrous webs for decolorization of methylene blue dye in wastewater treatment. *RSC Advances.* 2014;4:32249-55.
- Giese EC. Mining applications of immobilized microbial cells in alginate matrix: an overview. *Rev Int Contam Ambient.* 2020;36:775-87.
- Bashan LE, Bashan Y. Immobilized microalgae for removing pollutants: review of practical aspects. *Bioresour Technol.* 2010;101:1611-27.
- Cassidy MB, Lee H, Trevors JT. Environmental applications of immobilized microbial cells: a review. *J Ind Microbiol.* 1996;16:79-101.
- Vunain E, Mishra AK, Mamba BB. Dendrimers, mesoporous silicas and chitosan-based nanosorbents for the removal of heavy metal ions: a review. *Int J Biol Macromol.* 2016;86:570-58.
- Khongkhaem P, Intasiri A, Luepromchai E. Silica-immobilized *Methylobacterium* sp. NP3 and *Acinetobacter* sp. PK1 degrade high concentrations of phenol. *Lett Appl Microbiol.* 2011;52:448-55.
- Xia K, Ferguson RZ, Losier M, Tchoukanova N, Brüning R, Djaoued Y. Synthesis of hybrid silica materials with tunable pore structures and morphology and their application for heavy metal removal from drinking water. *J Hazard Mater.* 2010;183:554-64.
- Betiha MA, Moustafa YM, El-Shahat MF, Rafik E. Polyvinylpyrrolidone-Aminopropyl-SBA-15 Schiff Base hybrid for efficient removal of divalent heavy metal cations from wastewater. *J Hazard Mater.* 2020;397:122675.
- Gargiulo V, Alfè M, Lisi L, Manfredi C, Volino S, Di Natale F. Colloidal carbon-based nanoparticles as heavy metal adsorbent in aqueous solution: cadmium removal as a case study. *Water Air Soil Pollut.* 2017;228:192.
- Di Natale F, Gargiulo V, Alfè M. Adsorption of heavy metals on silica-supported hydrophilic carbonaceous nanoparticles (SHNPs). *J Hazard Mater.* 2020;393:122374.
- Baccile N, Babonneau F, Thomas B, Coradin T. Introducing ecodesign in silica sol-gel materials. *J Mater Chem.* 2009;19:8537-59.
- Ma JF, Yamaji N. Silicon uptake and accumulation in higher plants. *Trends Plant Sci.* 2006;11:392-7.
- Kalpathy U, Proctor A, Shultz J. Production and properties of flexible sodium silicate films from rice hull ash silica. *Bioresour Technol.* 2000;72:99-106.
- Stanojević-Nikolić S, Dimić G, Mojović L, Pejin J, Djukić-Vuković A, Kocić-Tanackov S. Antimicrobial activity of lactic acid against pathogen and spoilage microorganisms. *J Food Process Preserv.* 2016;40:990-8.
- Chen X, Tian Z, Cheng H, Xu G, Zhou H. Adsorption process and mechanism of heavy metal ions by different components of cells, using yeast (*Pichia pastoris*) and Cu^{2+} as biosorption models. *RSC Advances.* 2021;11:17080.
- Mrvčić J, Prebeg T, Barišić L, Stanzer D, Bačun-Družina V, Stehlik-Tomas V. Zinc binding by lactic acid bacteria. *Food Technol Biotechnol.* 2009;47:381-8.
- Yi Y-J, Lim J-M, Gu S, Lee W-K, Oh E, Lee S-M, et al. Potential use of lactic acid bacteria *Leuconostoc mesenteroides* as a probiotic for the removal of Pb(II) toxicity. *J Microbiol.* 2017;55:296-303.
- Gupta P, Diwan B. Bacterial exopolysaccharide mediated heavy metal removal: a review on biosynthesis, mechanism and remediation strategies. *Biotechnol Rep (Amst).* 2017;13:58-71.
- Ye G, Li G, Wang C, Ling B, Yang R, Huang S. Extraction and characterization of dextran from *Leuconostoc pseudomesenteroides* YB-2 isolated from mango juice. *Carbohydr Polym.* 2019;207:218-23.
- Zhao X, Yim C-H, Du N, Abu-Lebdeh Y. Shortly branched, linear dextrans as efficient binders for silicon/graphite composite electrodes in Li-ion batteries. *Ind Eng Chem Res.* 2018;57:9062-74.

37. Lowe BM, Skylaris C-K, Green NG. Acid-base dissociation mechanisms and energetics at the silica–water interface: an activationless process. *J Colloid Interface Sci.* 2015;451:231-44.
38. Zanoletti A, Ivano Vassura I, Venturini E, Monai M, Montini T, Federici S, et al. A new porous hybrid material derived from silica fume and alginate for sustainable pollutants reduction. *Front Chem.* 2018;6:1-13.
39. Carr FJ, Chill D, Maida N. The lactic acid bacteria: a literature survey. *Crit Rev Microbiol.* 2002;28:281-370.
40. Wang X-Y, Jiang X-P, Li Y, Zeng S, Zhang Y-W. Preparation Fe₃O₄@chitosan magnetic particles for covalent immobilization of lipase from *Thermomyces lanuginosus*. *Int. J. boil. Macromol.* 2015;75:44-5.
41. Sarwat F, Ul Qader SA, Aman A, Ahmed N. Production & characterization of a Unique Dextran from an Indigenous *Leuconostoc mesenteroides* CMG713. *Int J Biol Sci.* 2008;4(6):379-86.
42. Lesage G, Bussey H. Cell wall assembly in *Saccharomyces cerevisiae*. *Microbiol Mol Biol Rev.* 2006;70:317-43.
43. Staroń P, Chwastowski J. *Raphia*-microorganism composite biosorbent for lead ion removal from aqueous solutions. *Materials (Basel).* 2021;14:7482.
44. Tummino ML, Magnacca G, Dafne Cimino D, Laurenti E, Nisticò R. The innovation comes from the sea: chitosan and alginate hybrid gels and films as sustainable materials for wastewater remediation. *Int J Mol Sci.* 2020;21:550.
45. Moral CK, Yildiz M. Alginate production from alternative carbon sources and use of polymer based adsorbent in heavy metal removal. *Int J Polym Sci.* 2016;2:1-8.
46. De Gisi S, Lofrano G, Mariangela Grassi M, Notarnicola M. Characteristics and adsorption capacities of low-cost sorbents for wastewater treatment: a review. *Sustain. Mater. Technol.* 2016;9:10-40.